JOURNAL OF APPLIED ELECTROCHEMISTRY 26 (1996) 1217–1223

Aluminium alloys in sulfuric acid Part II: Aluminium–oxygen cells

S. MÜLLER, F. HOLZER, J. DESILVESTRO*, O. HAAS

Paul Scherrer Institut, Electrochemistry Section, CH-5232 Villigen PSI, Switzerland

Received 13 December 1995; revised 7 May 1996

Aluminium alloys were tested in Al/O_2 cells with strongly acidic electrolytes containing minor amounts of chloride ions. The faradaic efficiency, the maximum discharge capacity and the peak power of various Al/O_2 cells were evaluated. The temperature dependence of the faradaic efficiency was measured for an Al/O_2 cell over the temperature range from 15 to 50 °C. With a zinc-containing aluminium alloy, a faradaic efficiency of 84% and a cell voltage of 1.6 V at open circuit and 0.7 V at 100 mA cm^{-2} could be reached. The highest peak power 120 mW cm^{-2}, was obtained with an Al–Zn/Sn alloy. On the basis of the solubility of the anode products in the electrolyte, a limiting specific energy of 70 Wh kg^{-1} was estimated. The cell voltage depends on the Al-alloys and on the catalyst used in the oxygen electrode. The cell voltage could be increased by about 200 mV when replacing the Pt-catalysed oxygen electrode with a noble-metal-free (CoCAA/DCD) electrode.

1. Introduction

Because of its high specific energy and low electrode material cost, the Al/air battery is a good candidate for remote power supply and electric vehicle applications [1, 2].

To investigate the possible use of aluminium as an anode material in batteries for inexpensive electricity production, we previously investigated [3] Al/Cl_2 cells with porous graphite or Ti–Ti/Ru oxide [4] chlorine cathodes, using weakly acidic NaCl electrolytes and different additives like Zn, In and Hg [5, 6]. These additives shift the oxidation potential of the Al-anode closer to the thermodynamic potential (−1.6 V vs NHE). In combination with porous chlorine electrodes, cell voltages of about 2 V at 50 mA cm^{-2} could be achieved. Chlorine electrodes were used because of their predictable electrochemical behaviour. These promising results obtained with these cells encouraged us to investigate Al/O_2 cells in acidic electrolytes. It was necessary to increase the acid concentration considerably, however, in order to have a reasonable performance of the oxygen electrode. Highly acidic electrolytes lead to appreciable advantages over alkaline electrolytes such as: higher theoretical cell voltages [7], lower corrosion rates [8], and lack of carbonation problems for the air electrodes. One problem is that aluminium is passivated by a relatively thick oxide layer in concentrated H_2SO_4 solutions [9]. Fortunately, the addition of small amounts of Cl^- (or F^-) to the sulfuric acid leads to partial destruction of the oxide layer by pitting corrosion which activates the aluminium anode. Other additives such as Zn^{2+} and In^{3+} modify the Al surface and shift the anodic oxidation potential up to 400 mV closer to the thermodynamic potential of Al. Similar effects were observed by alloying the Al-99.99 with Zn, In or Sn. The electrochemical properties of different Al-alloys in electrolyte systems containing Cl^-, F^-, Zn^{2+} and In^{3+} additives have been described in detail in a previous publication [10]. That investigation discovered some promising electrode/electrolyte combinations for an Al/O_2 battery in acidic solutions. In the present paper we report on the behaviour of Al/O_2 cells in strongly acidic electrolytes. Voltage and power delivered by these cells were measured as functions of the current density. The faradaic efficiencies and discharge curves under constant load were determined for Al/O_2 cells using Al–Zn/In-, Al-Zn/Sn- and Al-99.5 (welding-rod quality) electrodes.

In anticipation of improving the cell performance, we also investigated the oxygen electrode behaviour in the electrolytes mentioned above. The Pt-catalysed O_2-electrode has been found to suffer from high overpotentials due to slow kinetics in acidic media [11], and also from catalyst poisoning by the halogen ions contained in the electrolyte [12]. In the present investigation, however, Teflon-bonded Co-catalysed oxygen electrodes were found not to exhibit this poisoning problem.

For the work described here, a single cell arrangement with 20 cm^2 electrodes was used. In another paper we have described a bipolar cell arrangement using 100 cm^2 electrodes [13].

2. Experimental details

2.1. *Cell components*

2.1.1. Anodes. All Al-alloys were based on Al-99.99 and were produced and provided by Alusuisse–Lonza Services AG (Switzerland), except for Al-99.5

* Present address: Leclanché SA, 48, Avenue de Grandson, CH-1400 Yverdon-les-Bains, Switzerland

0021-891X

(welding-rod quality). The following alloys were employed in this investigation (percentages are by weight): Al–In 0.10%, Al–Zn/In (3.3%/0.025%), Al–Zn/Sn (6.5%/0.16%) and Al-99.5% (for an analysis see [5]).

The Al-rods were machined to a diameter of 5 cm. Pretreatment of the circular endfaces used as the working surface consisted of mechanical polishing (600 SiC paper) followed by rinsing with deionized water.

(a) *Corrosion under load:* The weight loss of the anode in the cell is due to both the electrochemical reaction which delivers the current and the corrosion reaction which leads to hydrogen evolution. The hydrogen evolution rate at the Al-electrode was measured volumetrically during the discharge of the cell to determine the time dependency of the faradaic efficiency. The overall faradaic efficiency was calculated based on the ratio of the weight of the Al oxidized by the current drawn from the cell to the total weight loss of the anode after the run.

(b) *Open-circuit corrosion:* The corrosion rate of the anode was measured gravimetrically at open circuit potential (o.c.p.) by holding the Al-rods in either acidic or alkaline electrolyte solution.

2.1.2. Cathodes. The following cathodes were used:

(i) PTFE-bonded gas-diffusion electrodes obtained from Eltech, and having a Pt loading of $4\,mg\,cm^{-2}$ and a gold-plated silver mesh current collector. The thickness of the electrode was 0.64 mm.
(ii) PTFE-bonded two-layer gas-diffusion electrodes, with Pt loading of $0.4\,mg\,cm^{-2}$ and a Pt current collector, prepared in our laboratories (PSI) by the rolling technique described in a previous paper [14]. The thickness of the electrode was 0.5 mm.
(iii) PTFE-bonded two-layer gas-diffusion electrodes, with a mixture of cochloanilamide and dicyandiamide (CoCAA/DCD) catalyst (Co-loading: $3\,mg\,cm^{-2}$) and a Pt current collector, prepared in our laboratories by the same rolling technique [14]. The thickness of the electrode was 0.5 mm.

The current collector was embedded into the hydrophobic diffusion layer facing the gas supply chamber of the cell so as to avoid any electrochemical reaction at the current collector.

2.1.3. Electrolyte. Electrochemical experiments were carried out in 3 M H_2SO_4 (prepared with deionized H_2O from conc. H_2SO_4, Baker Chemicals, p.a.) with the following additives. $ZnSO_4 \cdot 7H_2O$ and $ZnCl_2$ were purchased from Merck (p.a. quality), $In_2(SO_4)_3 \cdot 5H_2O$ (purum) from Fluka. The total chloride concentration was adjusted by addition of HCl (Baker Chemicals, p.a.).

To study the impact of chloride ions on the activity of the oxygen reduction catalysts, current–potential curves of Pt-containing and Pt-free diffusion electrodes were measured in 3 M H_2SO_4 and in 3 M H_2SO_4 + 40 mM HCl. In the HCl-free electrolyte, a Pt-wire was used as the counter electrode. For the HCl-containing electrolyte, an Al-rod was used as the counter electrode in order to avoid chlorine gas evolution at the counter electrode.

2.2. *Apparatus*

The voltage and power of the cells were measured as functions of the current density by cell discharge through an external load that was varied from a starting load of 5.6 Ω to a final load of 0.1 Ω. The potential of each electrode against Hg/Hg_2SO_4 and the cell voltage were recorded as functions of time by a computer data acquisition system (National Instruments). For programming of the AD/DA data acquisition system the software tool LabWindows (National Instruments) was used.

2.3. *Cell design*

The Al/O_2 test cell is depicted in Fig. 1. The cell compartment was built with poly(methyl-methacrylate) (Plexiglas). The circular Al-anode face was placed parallel to the oxygen cathode. To contact the cathode to the external load, a platinum spiral was pressed against the backing layer of the current collector. The anode was contacted with an Al screw which

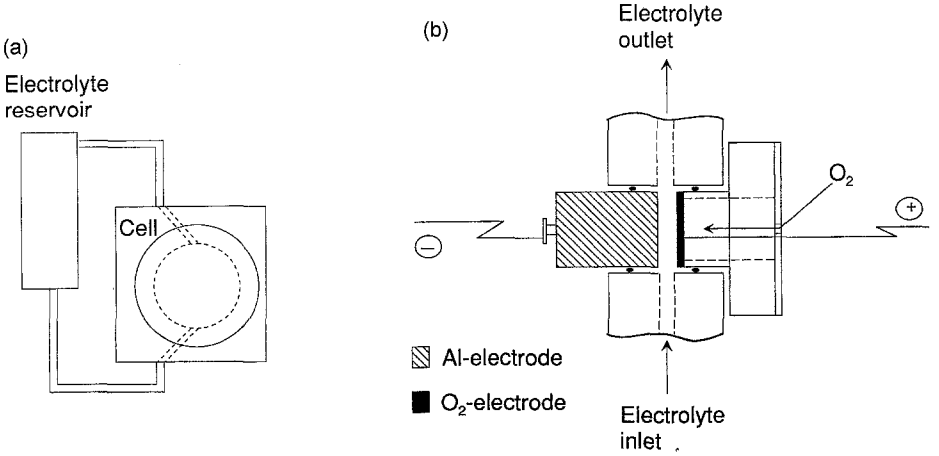

Fig. 1. Schematic view of the Al/O_2 cell. (a) Overview with electrolyte reservoir and (b) cell cross section.

Table 1. Corrosion rates of three different Al-alloys: Al–Zn/Sn, Al–Zn/In and Al–99.5 (welding-rod quality), exposed to 3 M H_2SO_4 + 40 mM HCl and to 4 M KOH. Exposed surface area: 20 cm^2

Al-alloy	*Corrosion rate (3 M H_2SO_4 + 40 mM HCl)*/mg min^{-1}	*Corrosion rate (4 M KOH)*/mg min^{-1}
Al–Zn/Sn	0.212	3.030
Al–Zn/In	0	2.485
Al–99.5	4.060	5.878

penetrated the back of the Al-electrode. The gap between the electrodes was adjusted to 3 mm. The geometrical surface area of the electrodes was 20 cm^2. The electrolyte was pumped from an external reservoir through the cell compartment by a hydrogen bubble pump using the parasitic hydrogen evolved on the aluminium anode. The faradaic efficiency was evaluated by measuring the rate of H_2 evolution at the Al-electrode and the current density at different times. The Al-electrode was thermostated with an external water circuit to either 19 °C or 50 °C. The temperature was controlled by a thermocouple inserted into the anode from the backside.

3. Results and discussion

3.1. *Corrosion currents and faradaic efficiencies*

3.1.1. Corrosion rates of Al–Zn/Sn, Al–Zn/In and Al-99.5 in acidic and alkaline solutions. The o.c.p. corrosion of Al–Zn/Sn, Al–Zn/In and Al–99.5 (welding-rod quality) was measured over a period of 5.5 h in 3 M H_2SO_4 + 40 mM HCl and, for comparison, in 4 M KOH, the results of which are shown in Table 1. Addition of 40 mM HCl to the 3 M H_2SO_4 was necessary to avoid passivation of the aluminium in this electrolyte. The surface area of the Al-rods was 20 cm^2. The results can be summarized as follows: (a) the corrosion rates of Al–Zn/Sn and Al–Zn/In were more than 14 times lower in 3 M H_2SO_4 + 40 mM HCl than in 4 M KOH, (b) Al-99.5 also showed a lower corrosion rate in highly acidic than in alkaline electrolytes, (c) Al–99.5 showed a higher corrosion rate than Al–Zn/Sn or Al–Zn/In in acidic as well as in alkaline electrolytes.

3.1.2. Faradaic efficiency of Al–99.5 anodes in acidic electrolytes. The faradaic efficiency and the cell voltage depend on the Al-alloy and on the electrolyte additives. Al–99.5 is used for welding-rods, this Al quality is reasonably pure and a low cost material which would be attractive for practical applications in batteries. Earlier experiments with rotating Al-discs in acidic solutions (3 M H_2SO_4) had shown a better faradaic efficiency when 80 mM Zn(II), 0.5 mM In(III) and 40 mM HCl were added to the electrolyte [15]. These additives make the Al-electrode potential about 250 mV more negative without increasing the chemical corrosion rate. We therefore used these additives also in the present investigation of Al–99.5 electrodes. With the electrochemical cell depicted in Fig. 1 and a constant external resistance, we measured the faradaic efficiency for four different sulfuric acid concentrations (5 M, 3 M, 1.5 M and 0.75 M) in the presence of the additives mentioned (80 mM Zn (II), 0.5 mM In (III), 40 mM HCl). To activate the Al-electrode in 5 M H_2SO_4 it was necessary to add 160 mM HCl instead of the usual 40 mM HCl. A porous oxygen diffusion electrode was used as the counter electrode. The results obtained for Al–99.5 are listed in Table 2 together with the cell voltage and associated current densities. With this cell arrangement, the highest faradaic efficiency (86%) and power density (ca. 90 mW cm^{-2}) was reached in 3 M H_2SO_4. In 1.5 M H_2SO_4 the Al-electrode potential was more positive and the internal resistance somewhat higher. In this electrolyte a faradaic efficiency of 71% was measured. At either lower or higher H_2SO_4 concentration (0.75 M and 5 M, respectively) the voltage and current delivered by the cells were lower still, but a faradaic efficiency of 81% could be measured. This rather inconsistent behaviour unfortunately cannot be explained. However, it demonstrates that with 3 M H_2SO_4 containing 80 mM Zn (II), 0.5 mM In (III) and 40 mM HCl a very promising power density at high faradaic efficiency is obtained.

Table 2. Comparison of cell voltage, current density and faradaic efficiency for Al–99.5 (welding-rod quality) anodes and Eltech O_2-cathodes in four different H_2SO_4 electrolyte solutions containing 40 mM Cl^-, 80 mM Zn^{2+} and 0.5 mM In^{3+} as the additives. Discharge time: 2.5 h

$c(H_2SO_4)$/M	U/V	i/mA cm^{-2}	η/%
5*	0.45	61	81
3	0.82	112	86
1.5	0.69	96	71
0.75†	0.59–0.39	80–50	81

* 160 mM HCl instead of 40 mM HCl.
† Cell voltage and current density decreased continously.

3.1.3. Faradaic efficiency of Al–Zn/In (3.3%/0.025%) and Al–Zn/Sn (6.5%/0.16%) alloys in acidic electrolytes. Earlier rotating-disc experiments with Al–Zn/In (3.3%/0.025%) and Al–Zn/Sn (6.5%/0.16%) alloys as the electrode material in acidic solutions showed reproducible faradaic efficiencies of about 90% for both alloys in 3 M H_2SO_4 with 80 mM Zn (II), 0.5 mM In (III) and 40 mM HCl [10]. For 3 M H_2SO_4, with only HCl as an additive, the faradaic efficiencies were 84% and 90% for the Al–Zn/In and Al–Zn/Sn electrodes, respectively. These results indicate that no significant improvement of the faradaic efficiency could be reached for these alloys by adding Zn(II) and In(III) to the electrolyte. Therefore, Al–Zn/In and Al–Zn/Sn, were used as anodes in the electrochemical cell depicted in Fig. 1 without the addition of Zn(II) and In(III) to the electrolyte. With the Al–Zn/In-electrode we obtained faradaic efficiencies between 72 and 84% in 3 M H_2SO_4 + 40 mM HCl (Table 3). For these experiments (measured with constant external load) the efficiency was

Table 3. Comparison of cell voltage, current density and faradaic efficiency of Al–Zn/Sn and Al–Zn/In anodes and Eltech O_2-cathodes after various discharge times, using two different external loads. The electrolyte was 3 M H_2SO_4 + 40 mM HCl. The cited load does not include the contact resistance to the cell, which varies between 50 and 240 mΩ

Al–alloy	*Discharge*/h	*U*/V	*i*/mA cm^{-2}	*η*/%	*Load*/Ω
Al–Zn/In	3.5	1.0	55	72	0.78
Al–Zn/In	8.0	0.95	75	81	0.43
Al–Zn/In	25	1.0	60	84	0.78
Al–Zn/Sn	3.5	1.0	60	77	0.78
Al–Zn/Sn	8.5	1.0	75	59	0.43
Al–Zn/Sn	25	1.1	55	44	0.78

measured as a function of time using the hydrogen evolution rate and the current–time curve. The measurements were made over periods of 3.5, 8 and 25 h. Higher hydrogen evolution rates were observed during the first few hours. Thus, the faradaic efficiency increased from 72% to 84% during the 25 h operation.

For the Al–Zn/Sn alloy, exactly the opposite corrosion behaviour was observed. The faradaic efficiency decreased significantly with operation time in 3 M H_2SO_4 + 40 mM HCl (Table 3). Figure 2(a) shows the development of the electrode potential and cell voltage with time using this Al–Zn/Sn alloy as an anode in the Al/O_2 cell depicted in Fig. 1. The behaviour of the cell current and corrosion current is shown in Fig. 2(b). It is striking that the corrosion current develops in two steps, the first step from 0–20 mA cm^{-2} occurring within the first hour and the second step from 20–60 mA cm^{-2} occurring after the fourth hour. The corrosion behaviour seems to be influenced by the dissolution of alloying elements into the electrolyte. In the case of Al–Zn/In alloy, the hydrogen evolution is inhibited by the dissolved elements and the faradaic efficiency therefore increases with time. Whereas, the Zn^{2+} and Sn^{2+} which are dissolving from the Al–Zn/Sn alloy seem to catalyse the hydrogen evolution. When the Al–Zn/Sn/O_2 cell was connected to a 0.43 Ω resistance, the anode potential first dropped to −1.2 V, then it slowly decreased further to −1.45 V vs Hg/Hg_2SO_4 while the cell potential increased to about 1 V (Fig. 2(a)). After the first corrosion current step, a faradaic efficiency of about 80% was reached, after the second step it decreased to 60% and after 25 h (Table 3) it was only about 45%.

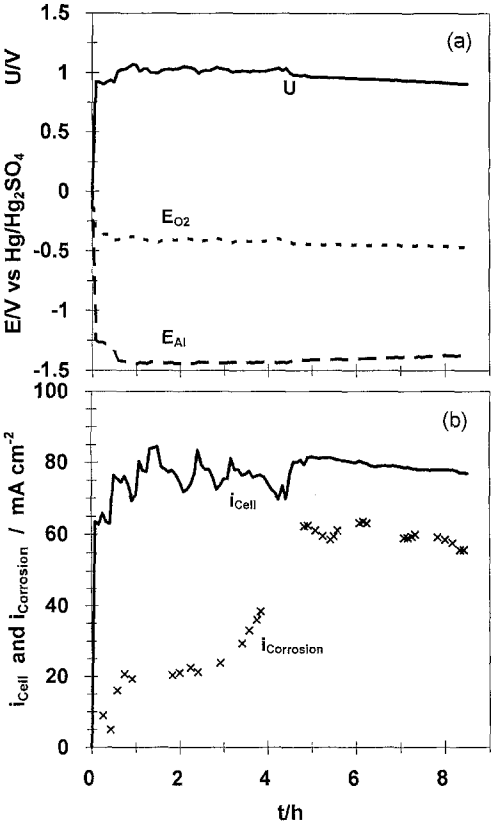

Fig. 2. (a) Cell voltage and electrode potentials, (b) current density and corrosion current density, as functions of time for an Al/O_2 cell using Al–Zn/Sn as the anode and an Eltech oxygen electrode as the cathode. The electrolyte was 3 M H_2SO_4 + 40 mM HCl.

3.2. *Temperature dependence of the faradaic efficiency*

The temperature dependence of the faradaic efficiency has not been investigated extensively, but the following experiments may give an idea as to how much the faradaic efficiency can be influenced by the temperature. The temperature dependence of the faradaic efficiency was measured using an Al–Zn/In (3.3%/0.025%) alloy electrode with a water flow-through cooling and heating system and 0.43 Ω as an external resistance (Table 4). We measured a faradaic efficiency of about 89% when the electrode was kept at 20 °C, and about 65% when it was thermostated to 50 °C, while the cell current was about 75 mA cm^{-2}. Without active cooling or heating of the Al–Zn/In-electrode, the temperature slowly increased to about 38 °C due to the heat produced with the currents reported in Table 4, whereas the electrolyte temperature only increased from 21 to 24 °C, for an experiment of 8 h (Fig. 3). Without active cooling we measured a faradaic efficiency of about 81%, which corresponds to the values in Table 3 for the earlier experiment. These experiments show that corrosion (hydrogen evolution) can be suppressed, and thus the faradaic efficiency increased, when the electrode is cooled. In practical cell without

Table 4. Comparison of current density, corrosion current density, temperature of the electrolyte and temperature of the Al–Zn/In anode, with and without thermostatic control of the anode. Eltech O_2-cathodes were used in these measurements

Thermostated	$T_{electrolyte}$ /°C	T_{Al} /°C	$i_{corrosion}$ /mA cm^{-2}	*i* /mA cm^{-2}	*η*/%
No temperature control	21–24	22–38	15	75	81
Heated Al-electrode	22–31	50–52	30	75	65
Cooled Al-electrode	21–22	15–19	5	55	89

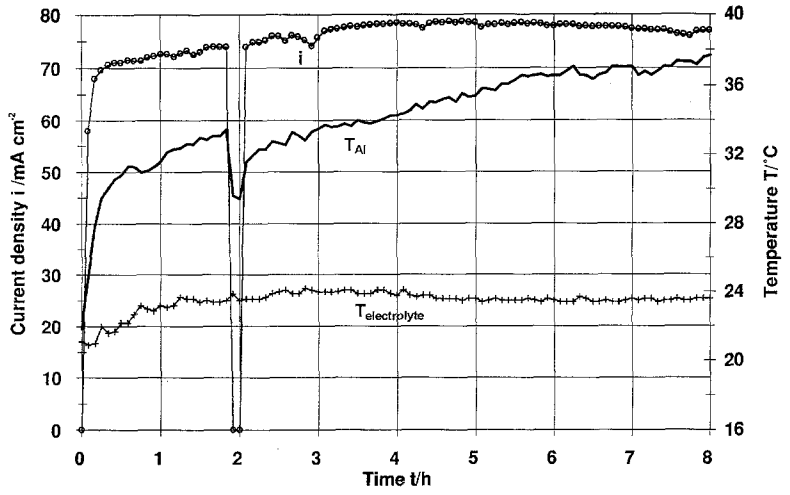

Fig. 3. Development of current and temperature with time for an Al/O_2 cell using Al–Zn/In as the anode and an Eltech oxygen electrode as the cathode. Discharge current (○), temperature of the anode (—) and temperature of the electrolyte (+). Electrolyte: 3 M H_2SO_4 + 40 mM HCl. External resistance: 0.43 Ω.

temperature control of the anode, the stationary temperature established at the Al-electrode depends on the current density. At high current densities the electrode temperature can be significantly higher than the electrolyte temperature, and the corrosion rate in this case increases due to the increase of electrode temperature. Heat production at the anode is expected since the electrochemical oxidation of the Al-anode occurs only at an overpotential of more than 1 V. This, in fact, could be an additional explanation for the so-called negative difference effect [16], which obtained its name due to the unexpected observation that the corrosion rate (hydrogen evolution rate) at an Al-electrode increases with increasing electrode potential and faradaic current, whereas at a noble metal electrode the hydrogen evolution is expected to decrease with increasing electrode potential. The negative difference effect at Al-electrodes could result from the increase in electrode temperature with increasing current density. The electrode works at high overpotential and therefore produces heat. The expected increase of the faradaic efficiency at higher current (more positive potential) may therefore be compensated by a decrease of the faradaic efficiency on account of the higher electrode temperature.

3.3. *Current–potential and power density curves of the Al/O_2 cells*

We measured the current–potential and power density curves of the Al/O_2 cell depicted in Fig. 1 with four different Al-anodes using 3 M H_2SO_4 + 40 mM HCl as an electrolyte. The cell characteristic of the Al/O_2 cell strongly depends on the anode material, as can be seen from Fig. 4. The highest potentials (at current densities up to 125 mA cm^{-2}) were obtained with an Al–In 0.10 alloy. At higher current densities the Al–Zn/Sn alloy showed the best performance. The lowest cell potential was obtained with Al–99.99. The highest peak power was measured for Al–Zn/Sn (120 mW cm^{-2} at a current density of 165 mA cm^{-2} and a voltage of 0.75 V).

At low current densities the main part of the voltage decay occurring with increasing current density is caused by slow kinetics at the oxygen electrode, whereas at higher current densities the *iR* drop in the cell is more important. The internal resistance of the cell was about 150 mΩ, according to the slope of the current–potential curve.

3.4. *Capacity and energy density of the acidic Al/O_2 cell*

The capacity and the energy density of the Al/O_2 cell depend on the maximum aluminium salt concentration which can be reached in the electrolyte solution. In acidic electrolytes, protons are consumed at the oxygen electrode and the anions of the acid are used to form a more or less soluble aluminium salt. A strong pH increase and precipitation of $Al(OH)_3$ accompanied by passivation of the electrode are expected as soon as the acid is consumed. The capacity of an acidic Al/O_2 battery, therefore, depends on the volume of the electrolyte reservoir, the concentration of the acid at the beginning of the discharge process, the solubility of the Al-salt formed, and the faradaic efficiency of the electrochemical aluminium dissolution process. Since the aluminium

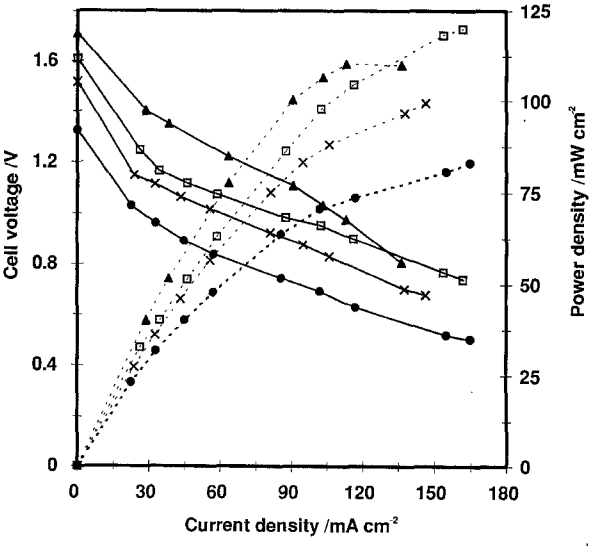

Fig. 4. Voltate (—) and power density (– – –) against current density for Al/O_2 cells using Al–In (▲), Al–Zn/Sn (□), Al–Zn/In (×) or Al–99.99% (●) as anodes. Al and O_2 (Eltech) electrode surface areas: 20 cm^2. Electrolyte: 3 M H_2SO_4 + 40 mM HCl.

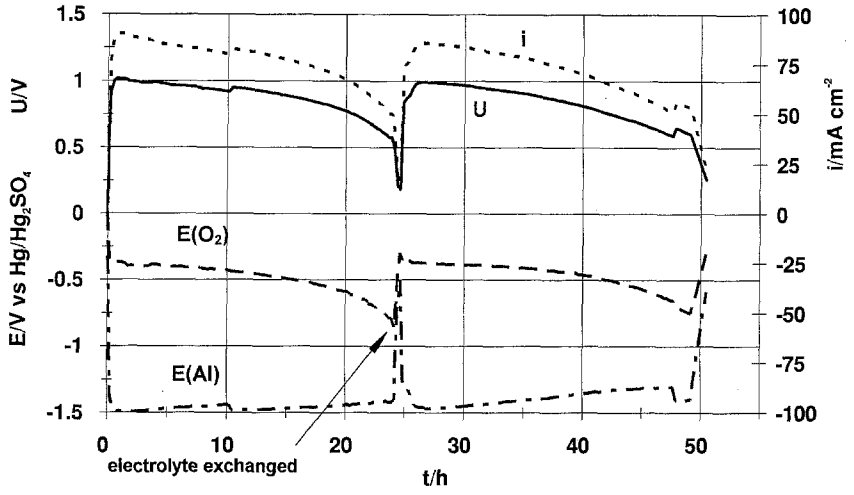

Fig. 5. Voltage and current density as functions of time for an Al/O_2 cell using Al–Zn/Sn as the anode and an Eltech oxygen electrode as the cathode. Electrolyte: 3 M H_2SO_4 + 40 mM HCl; Electrolyte volume: 400 ml. The electrolyte was exchanged after 25 h.

ions are formed at the electrode surface, the precipitation of aluminium salt may start at the electrode surface before the whole electrolyte solution is saturated. An experimental evaluation of these quantities is therefore necessary.

The time dependence of the cell voltage and the current at constant external load (0.43 Ω) served to measure the experimental Al-salt dissolving capacity (in Ah) for a given electrolyte volume. The results of these measurements carried out with 400 ml of 3 M H_2SO_4 + 40 mM HCl and the Al–Zn/Sn alloy electrode are shown in Fig. 5. After a short induction time a cell voltage of about 1 V and a current of about 80 mA cm^{-2} was reached. Cell voltage and current then decreased very slowly to about 60% of these values before a sudden decrease of the cell voltage and current occurred after about 25 h. At this time the aluminium concentration was 1.5 M, which means that about 3/4 of the acid was used up. The specific conductivity of the electrolyte was 130 mS cm^{-1} at this point.

The cell performance could be reproduced after replacing the spent electrolyte by 400 ml of a fresh solution containing 3 M H_2SO_4 + 40 mM HCl (second part of Fig. 5). The potentials of the oxygen electrode and Al-electrode measured against a Hg/Hg_2SO_4 reference electrode are shown in the lower part of Fig. 5.

The overall faradaic efficiency in this experiment was 65%. With these results the upper limits of the charge and energy density of an Al/O_2 battery can be estimated. Using 3 M H_2SO_4 + 40 mM HCl and the Al–Zn/Sn alloy electrode, the charge density and energy density are limited by the electrolyte to values of about 80 Ah dm^{-3} and about 95 Wh dm^{-3}, respectively. Preliminary tests have shown that a higher energy density could not be achieved by adding concentrated H_2SO_4 to the electrolyte reservoir. The formed $Al_2(SO_4)_3$ consumes high amounts of H_2O [19], thus a compact gel inhibits further cell operation.

The energy density values evaluated here, however, are only based on the electrolyte solution and do not include any other cell components. In fact, it is the limit of the energy density, which can be reached in a small Al/O_2 cell with a large electrolyte reservoir.

3.5. *Catalyst for the oxygen electrode*

The theoretical potential of an acidic Al/O_2 battery is 2.95 V [8]. In practice this value is never achieved, in fact only about 1–1.7 V are obtained. The most important loss comes from the aluminium electrode, which works at a considerable overpotential. As has been shown before, these losses can be reduced when using special alloys or electrolyte additives. However, a significant improvement of the cell voltage should also be possible if the oxygen electrode is optimized. In our electrolyte, unfortunately, the platinum-catalysed O_2-electrode has a higher overpotential for oxygen reduction than expected, which is due to the chloride ions needed to activate the aluminium electrode. Cl^- adsorption on the Pt catalyst is detrimental to the catalytic activity of the platinum and shifts the working potential of the oxygen electrode to more negative values. The Pt deactivated by Cl^- can be overcome using Cl^- insensitive, nonnoble metal catalysts such as Co or Fe-porphyrins and phthalocyanines. It has been shown that heat-treated metal macrocyles exhibit high activity for oxygen reduction, especially in acidic media [17]. A new, Co-based catalyst which is almost insensitive to Cl^- ions has recently been developed using a mixture of Co-chloranilamide and dicyandiamide (CoCAA/DCD) and Vulcan XC 72 which was pyrolysed at 850 °C in nitrogen [18]. To test this catalyst we prepared a porous gas-diffusion electrode using CoCAA/DCD with 3 mg Co cm^{-2}, and compared this electrode with a commercial Pt-catalysed gas-diffusion electrode (Eltech 4 mg Pt cm^{-2}) and a Pt-catalysed gas-diffusion electrode fabricated at PSI with 0.4 mg Pt cm^{-2}. The two-layer Teflon®-bonded electrodes were prepared by the rolling technique described before [14]. The current–potential curves of these three electrodes were measured in pure 3 M H_2SO_4 (Fig. 6(a)) and in 3 M H_2SO_4 + 40 mM HCl (Fig. 6(b)). Our electrodes, which were not yet optimized, showed a ~100 mV higher polarization than the Eltech electrode at current densities <30 mA cm^{-2}. The influence of the *iR* drop in the electrode is clearly noticeable at current densities above 30 mA cm^{-2}. After adding 40 mM HCl to 3 M H_2SO_4,

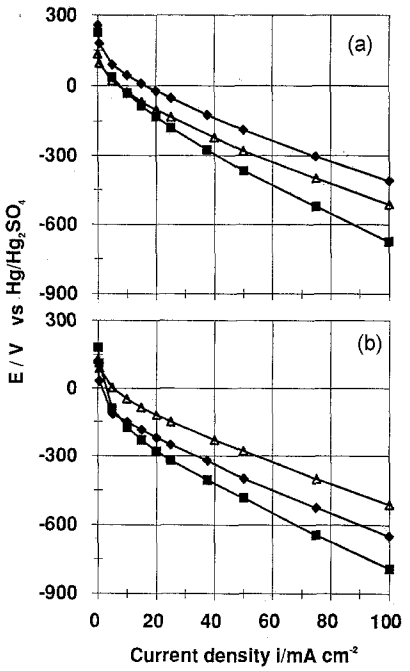

Fig. 6. Current–potential curves for O_2-electrodes. (■) PSI-electrode with 0.4 mg Pt cm^{-2}, (◆) Eltech electrode with 4 mg Pt cm^{-2} and (Δ) CoCAA/DCD-catalysed electrode with 3 mg Co cm^{-2}, measured in (a) pure 3 M H_2SO_4 and (b) 3 M H_2SO_4 + 40 mM HCl.

no deactivation of the CoCAA/DCD-catalysed electrode was detected, while a decrease of 120–240 mV in the oxygen reduction potential was recorded for the Pt-catalysed electrodes. In this Cl^- containing electrolyte, the CoCAA/DCD-catalysed electrode had the best current–potential behaviour of the three electrodes. This demonstrates that for this chloride-containing electrolyte the Pt-catalysed oxygen electrodes are not the best choice, and that the behaviour of the acidic Al/O_2 battery can be improved by using chloride-insensitive catalyst.

4. Conclusion

Based on our previous, more fundamental studies on Al and Al-alloys in highly acidic electrolytes, this paper reports results obtained with complete Al/O_2 cell systems. The shifts of the current–potential curves induced by various alloying elements are comparable to the results of our previous rotating disc measurements [10]. The faradaic efficiencies strongly depend on the cell operating conditions. We found faradaic efficiencies increasing with discharge time (up to 84%) for Al-alloys containing Zn and In, while the faradaic efficiency decreased for Al–Zn/Sn alloys during prolonged discharge times. The corrosion rates of all alloys tested were smaller in acidic than in alkaline electrolytes. With our cell arrangement the temperature of the Al-electrode increased during the experiment whereas the electrolyte temperature remained fairly constant. The increased electrode temperature results in lower faradaic efficiencies. The hydrogen produced may represent a serious safety problem for practical applications of this battery. Further improvement of the faradaic and energy efficiency may be realized by cooling the anode at high discharge currents and by reducing the polarization at the oxygen liberating-electrode. A CoCAA/DCD-catalysed oxygen electrode showed a promising current-potential characteristic with lower polarization than Pt-catalysed electrodes. The CoCAA/DCD catalyst is not poisoned by the chloride ions used to activate the aluminium electrode.

Acknowledgement

We acknowledge Nationaler Energie-Forschungs-Fonds for supporting this work (NEFF-Projekt 382). We thank Dr T. Allmendinger, ETH, for providing a sample of the CoCAA/DCD catalyst.

References

[1] J. F. Cooper, Lawrence Livermore Laboratory, UCRL-83881 (1980).
[2] S. Zaromb, *J. Electrochem. Soc.* **109** (1962) 1125.
[3] J.-F. Equey, S. Müller, A. Tsukada and O. Haas, *J. Appl. Electrochem.* **19** (1989) 65.
[4] *Idem, ibid.* **19** (1989) 147.
[5] G. Burri, W. Luedi and O. Haas, *J. Electrochem. Soc.* **136** (1989) 2167.
[6] J.-F. Equey, S. Müller, J. Desilvestro and O. Haas, *ibid.* **139** (1992) 1499.
[7] J. Jindra, J. Mrha and M. Musilova, *J. Appl. Electrochem.* **3** (1973) 297.
[8] M. Pourbaix, 'Atlas of Electrochemical Equilibria in Aqueous Solutions', 2nd edn, NACE Texas (1974) p. 168.
[9] R. Kötz, B. Schnyder and C. Barbero, *Thin Solid Films* **233** (1993) 63.
[10] F. Holzer, S. Müller, J. Desilvestro and O. Haas, *J. Appl. Electrochem.* **23** (1993) 125.
[11] D. B. Sepa, M. V. Vojnovic and A. Damjanovic, *ESC Ext. Abstr., 82-1* (no. 675, Spring 1982) 1077–78.
[12] M. T. Paffett, A. Redondo and S. Gottesfeld, Proceedings of the 2nd Symposium on Electrode Materials and Processing for Energy Conversion and Storage, The Electrochemical Society, Proceedings 87–12, (1987) p. 268.
[13] M. Rota, Ch. Comninellis, S. Müller, F. Holzer, O. Haas, *J. Appl. Electrochem.* **25** (1995) 114.
[14] S. Müller, K. A. Striebel and O. Hass, *Electrochim. Acta* **39** (1994) 1661.
[15] F. Holzer, S. Müller and J. Desilvestro, TM-51-90-28 (PSI internal report).
[16] A. R. Despic, D. M. Drazic, M. M. Purenovic and N. Cikovic, *J. Appl. Electrochem.* **6** (1976) 527.
[17] M. Ladouceur, G. Lalande, D. Guay, J. P. Dodelet, L. Dignard-Bailey, M. L. Trudeau, R. Schulz, *J. Electrochem. Soc.* **140** (1993) 1974.
[18] Th. Allmendinger, Diss. Eidgenössische Technische Hochschule (ETH), Zürich, Switzerland, nr. 9910 (1992).
[19] S. Schönherr, H. Görz, D. Müller, W. Gessner, *Z. Anorg. Allg. Chem.* **476** (1981) 188.